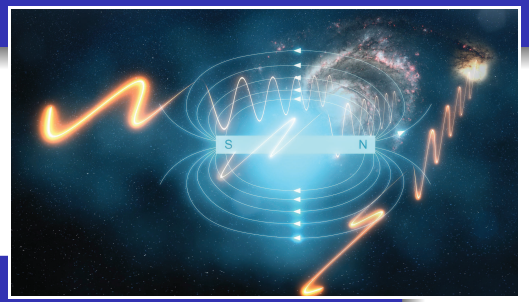

Magnetic fields in the Milky Way

Katia FERRIÈRE

Institut de Recherche en Astrophysique et Planétologie,
Observatoire Midi-Pyrénées, Toulouse, France

Cosmic Ray Anisotropy Workshop 2019

L'Aquila – October 7-11, 2019

Outline

1. Dust polarization
2. Faraday rotation
3. Synchrotron emission
4. Faraday tomography

Outline

1 Dust polarization

2 Faraday rotation

3 Synchrotron emission

4 Faraday tomography

Polarization direction

- Dust-extinct starlight *(optical)* is polarized $\parallel \vec{B}_\perp$
- Dust thermal emission *(infrared)* is polarized $\perp \vec{B}_\perp$

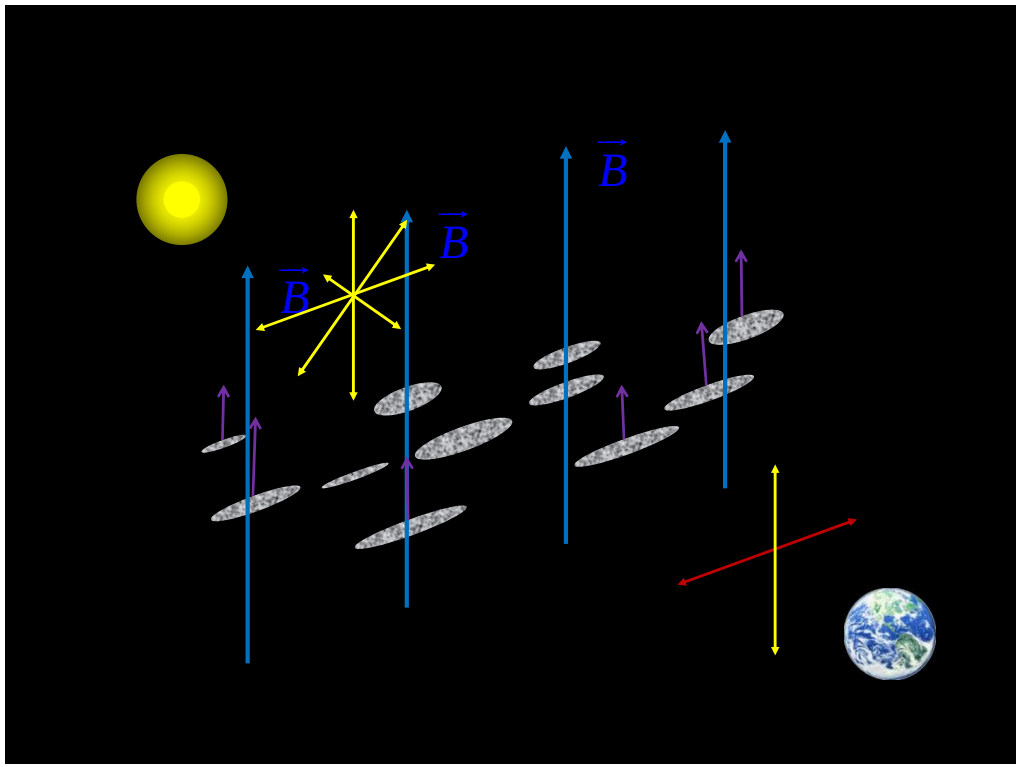

Figure Credit: *Philippe Terral*

Polarization fraction

- Dust-extinct starlight : $p \equiv \frac{P}{I} \simeq \tau\, p_0 \cos^2\gamma$
- Dust thermal emission : $p \equiv \frac{P}{I} = p_0 \cos^2\gamma$

$\hookrightarrow\ p_0 = p_{\max}\, F_{\rm align}\, F_{\delta B}$

$\vec{B} \in$ POS

$\left(\cos^2\gamma = 1\right)$

$\Rightarrow\ p = p_0$

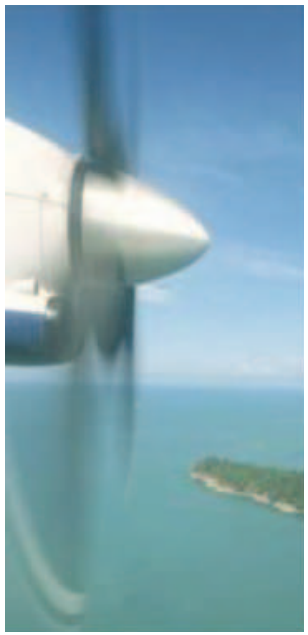

$\vec{B} \perp$ POS

$\left(\cos^2\gamma = 0\right)$

$\Rightarrow\ p = 0$

Credit: *Vincent Guillet*

Dust polarization

Altogether

- Polarization *direction* ☞ *orientation* of $\vec{B}$ *in* POS
- Polarization *fraction* ☞ *inclination* of $\vec{B}$ *to* POS (for ideal conditions)

Polarization of starlight

$\vec{B}_\perp$ segtors from 8 662 stars

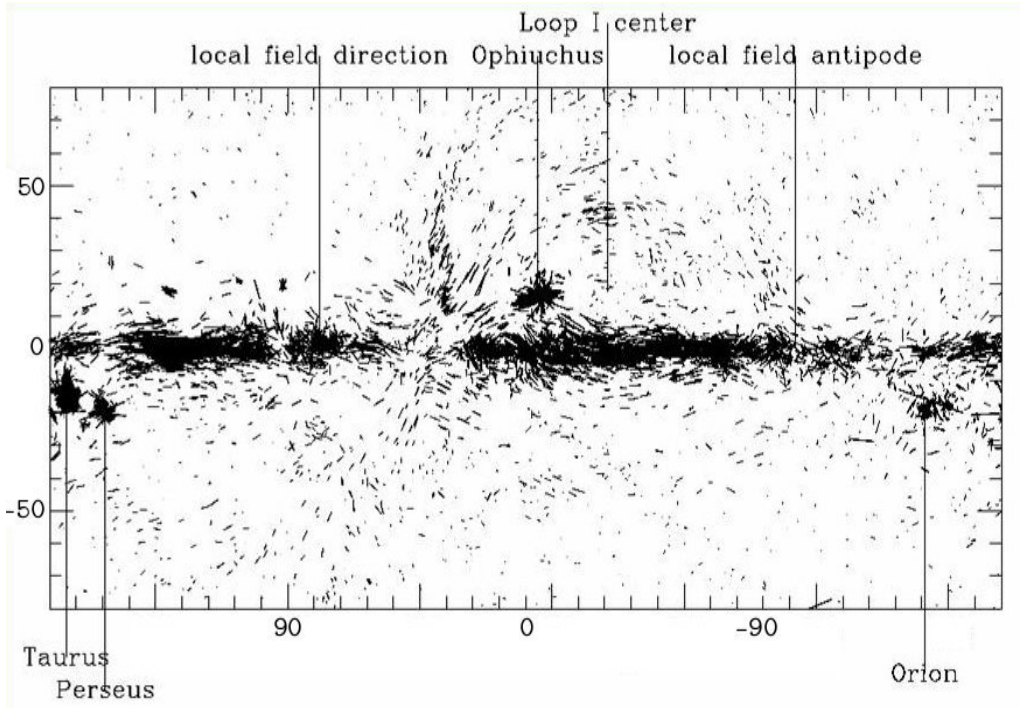

Heiles (2000)

☞ Near the Sun - In the disk : $\vec{B}_{\rm ord}$ is horizontal

$\vec{B}_{\rm ord}$ is nearly azimuthal ($p \simeq -7°$)

- In the halo : $\vec{B}_{\rm ord}$ has a vertical component

Polarization of dust thermal emission

Total intensity & $\vec{B}_\perp$ segtors at 353 GHz

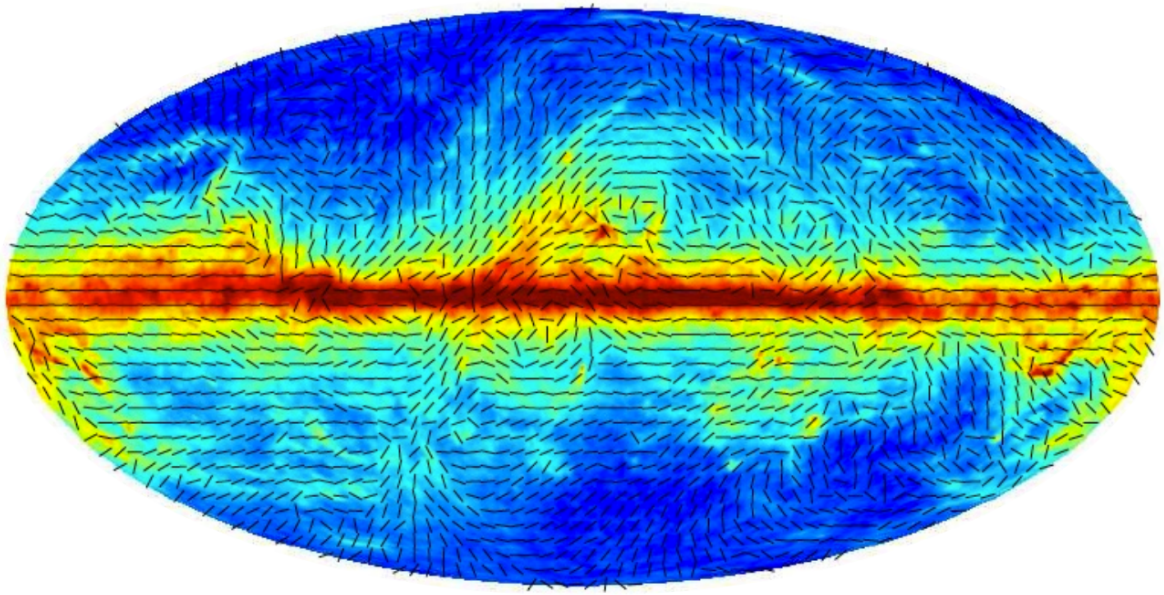

Planck collaboration (2015)

☞ - In the disk : $\vec{B}_{\rm ord}$ is horizontal

- In the halo : $\vec{B}_{\rm ord}$ has a vertical component

Polarization of dust thermal emission

Polarization fraction at 353 GHz

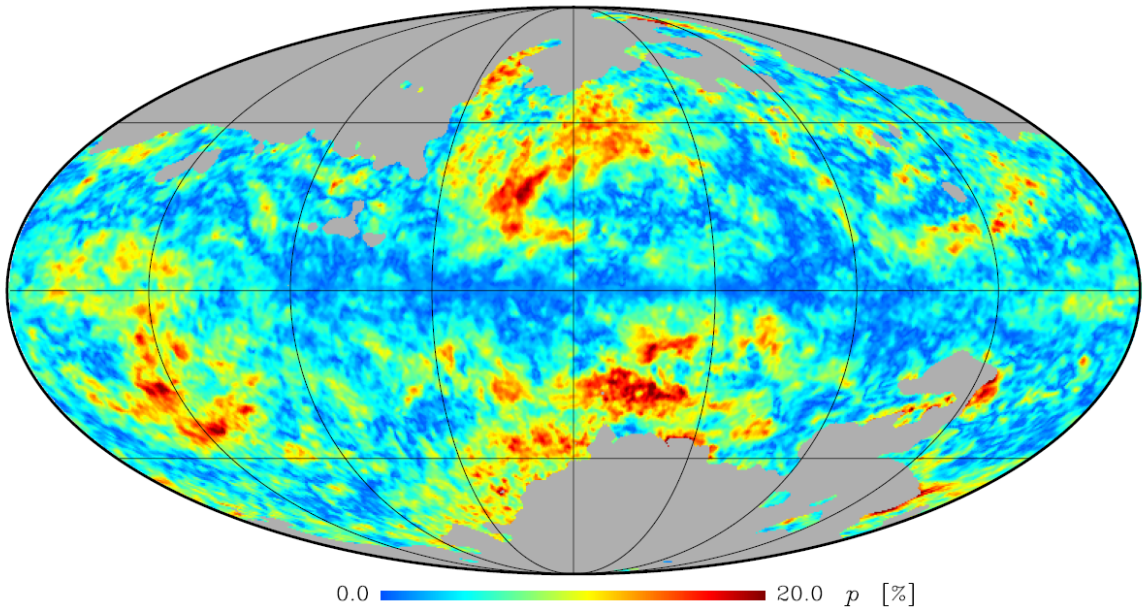

Planck collaboration (2015)

☞ Info on - Inclination of $\vec{B}_{\rm ord}$ to POS : $\cos^2\gamma$

- Magnetic fluctuations : $\frac{B_{\rm fluct}}{B_{\rm ord}}$

- Grain properties & alignment efficiency : $p_{\rm max}$ & $F_{\rm align}$

Polarization of dust thermal emission

Pipe Nebula at 353 GHz

I

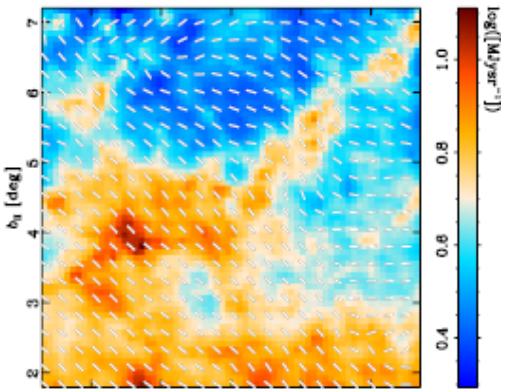

P

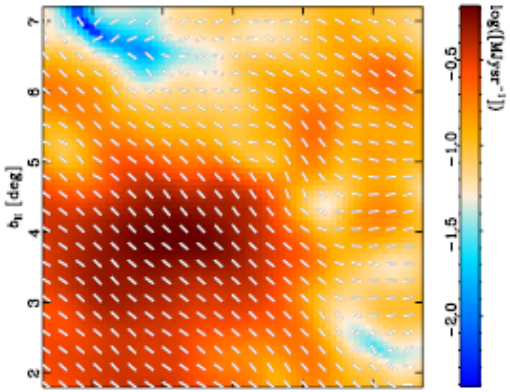

$p = \frac{P}{I}$

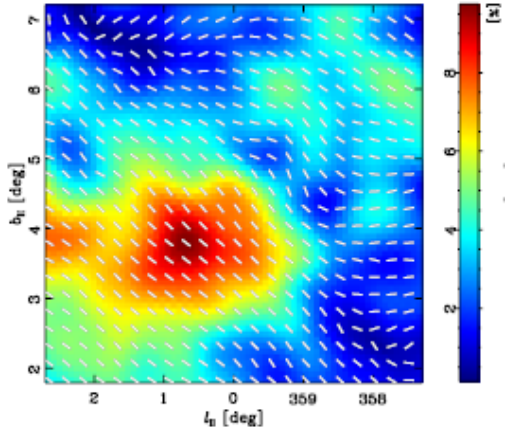

Planck collaboration (2015)

☞ Anti-correlation between $p = \frac{P}{I}$ & $\mathcal{S} = \sqrt{\langle(\Delta\psi)^2\rangle}$

Outline

1 Dust polarization

2 Faraday rotation

3 Synchrotron emission

4 Faraday tomography

Rotation measure

$\Delta\psi = \mathrm{RM}\ \lambda^2$ where $\mathrm{RM} = C \int n_\mathrm{e}\ B_{||}\ ds$

☞ $B_{||}$ in ionized regions

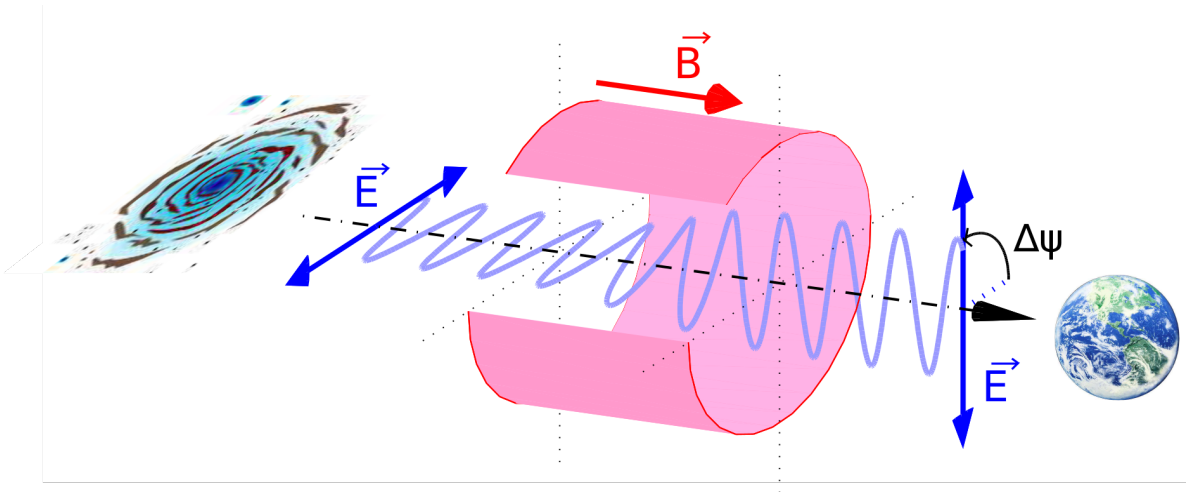

Figure Credit: *Philippe Terral*

Rotation measure

$$\Delta\psi = \mathrm{RM}\ \lambda^2 \quad \text{where} \quad \mathrm{RM} = C \int n_\mathrm{e}\ B_{||}\ ds$$

☞ $B_{||}$ in ionized regions

RMs of pulsars & EGRSs with $|b| < 8°$

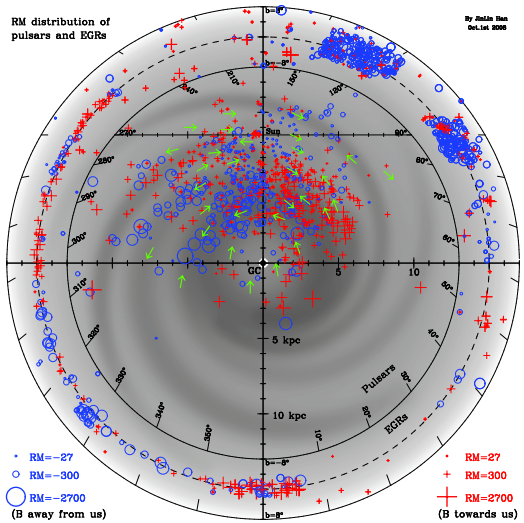

Han (2009)

RMs of EGRSs [NVSS ($\delta > -40°$) + S-PASS ($\delta < 0°$)]

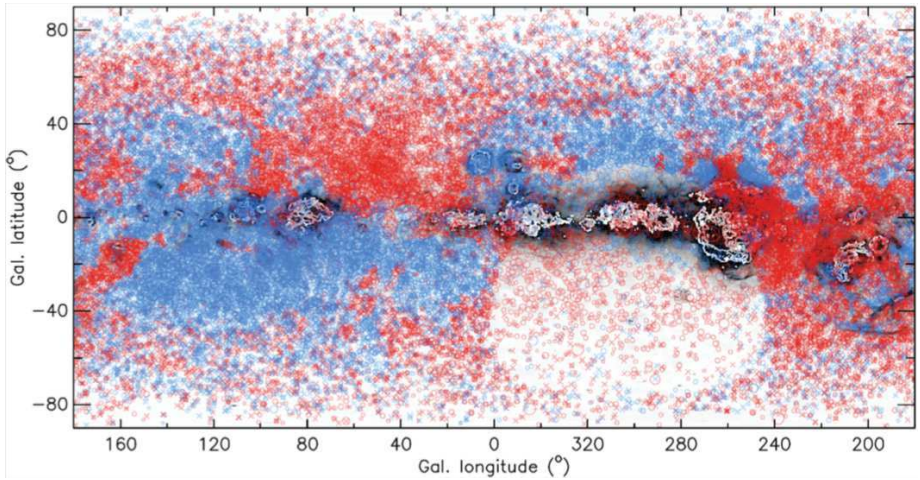

Schnitzeler et al. (2019)

Regular magnetic field

In ionized regions

- Near the Sun
  - $B_{\rm reg} \simeq 1.5\ \mu$G vs $\delta B_{\rm rms} \sim 5\ \mu$G
  - $\vec{B}_{\rm reg}$ is CW ($p \simeq -8°$)
- In the disk
  - $\vec{B}_{\rm reg}$ is horizontal & mostly azimuthal
  - $\vec{B}_{\rm reg}$ reverses direction with decreasing radius
  - $\vec{B}_{\rm reg}$ is symmetric in z
- In the halo
  - $\vec{B}_{\rm reg}$ has horizontal & vertical components
  - $\vec{B}_{\rm reg}$ is CCW at $z > 0$ & CW at $z < 0$
    $\rightarrow$ anti-symmetric in z
  - $(B_{\rm reg})_z \simeq +0.3\ \mu$G toward SGP & $\simeq 0\ \mu$G toward NGP
    $\rightarrow$ possibly consistent with symmetric disk field & anti-symmetric halo field

Regular magnetic field

Model of the large-scale magnetic field in the Galactic disk

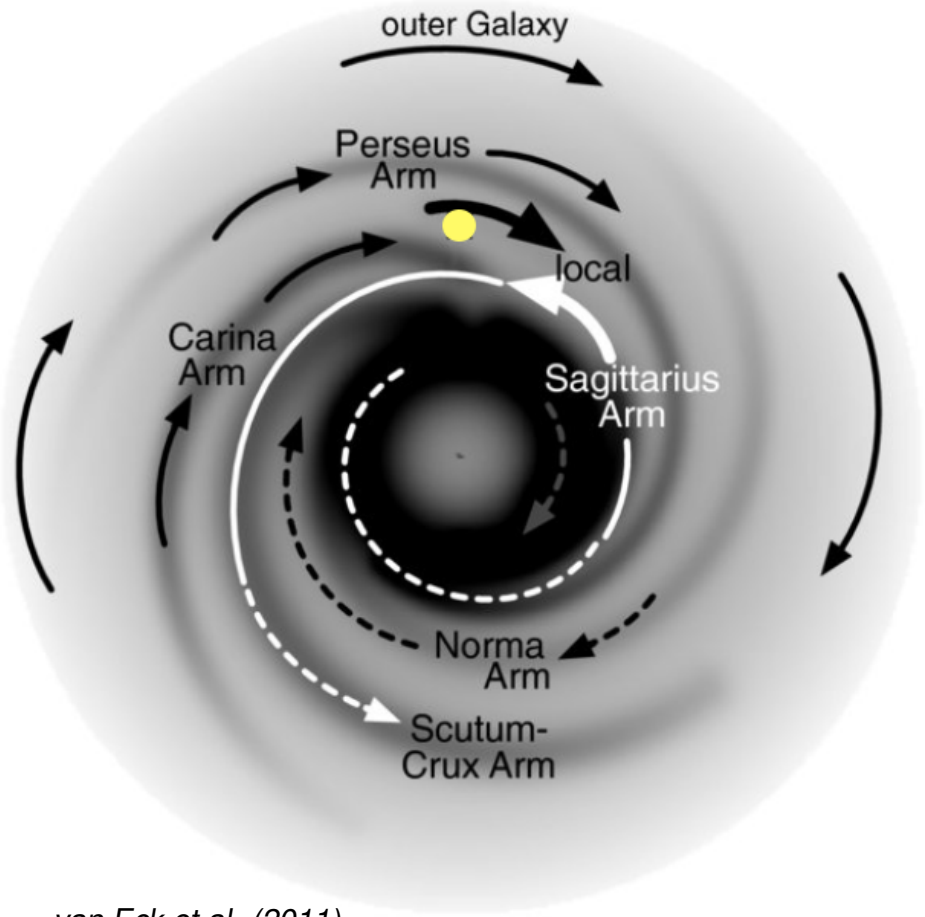

van Eck et al. (2011)

Regular magnetic field

Models of the large-scale magnetic field in the Galactic disk & halo

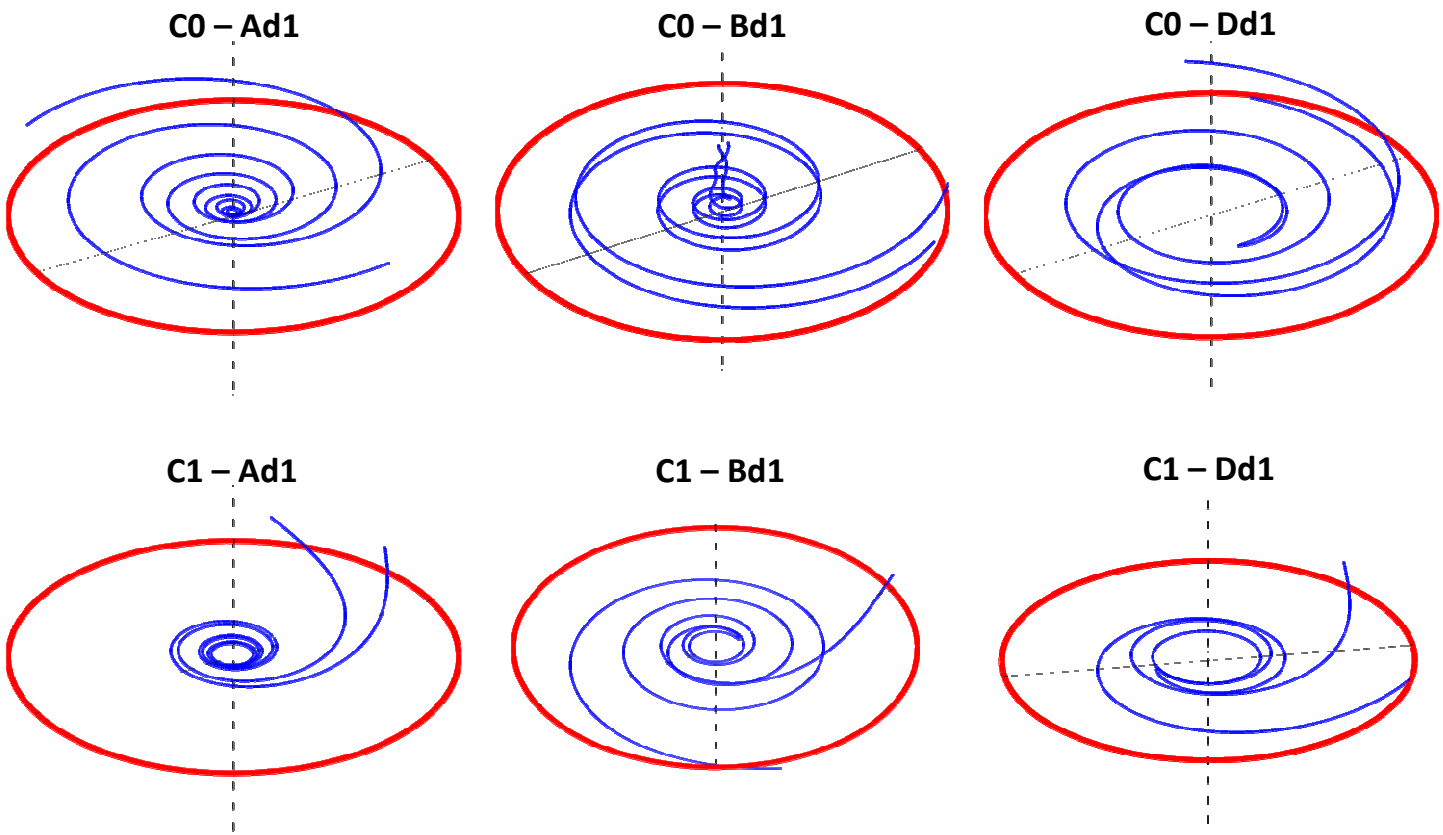

Terral & Ferrière (2017)

Fluctuating magnetic field

Statistical tools

- Auto-correlation function

$$C_F(\vec{r}) = \left\langle F(\vec{r}_1) \cdot F(\vec{r_2}) \right\rangle, \qquad \vec{r} = \vec{r_1} - \vec{r_2}$$

- Structure function *(better for irregularly spaced sources)*

$$D_F(\vec{r}) = \left\langle \left[F(\vec{r}_1) - F(\vec{r_2}) \right]^2 \right\rangle$$

$$\Rightarrow D_F(\vec{r}) = 2 \left[C_F(0) - C_F(\vec{r}) \right]$$

- Power spectrum

$$P_F(\vec{k}) = \frac{1}{(2\pi)^3} \int C_F(\vec{r}) \exp\left(-i\vec{k} \cdot \vec{r}\right) d\vec{r}$$

$$\Rightarrow \langle F^2 \rangle = \int P_F(\vec{k}) \, d\vec{k} = \int E_F(k) \, dk$$

Power spectrum from extragalactic RMs

Combine measured $\mathrm{RM} = C \int n_\mathrm{e}\, B_{\parallel}\, ds$ & $\mathrm{EM} = \int n_\mathrm{e}^2\, ds$

to derive power spectra of δn_e and δB separately *(Minter & Spangler 1996)*

Structure function of RM

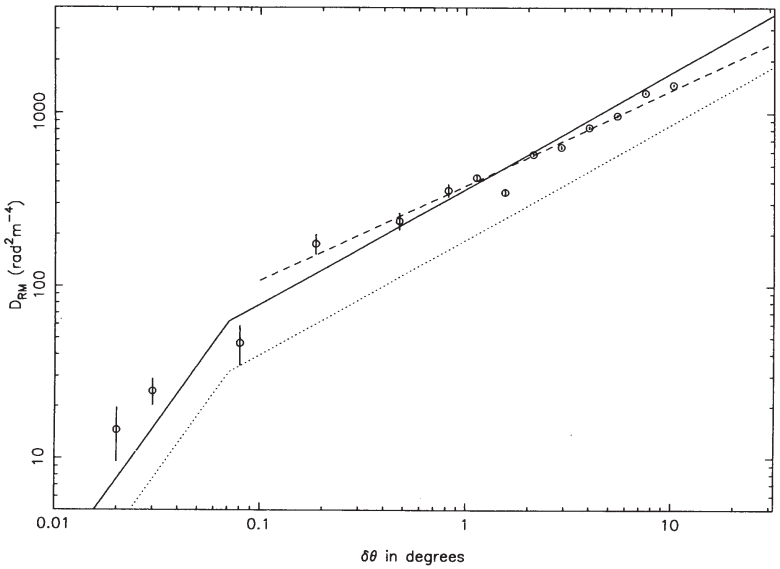

Structure function of EM

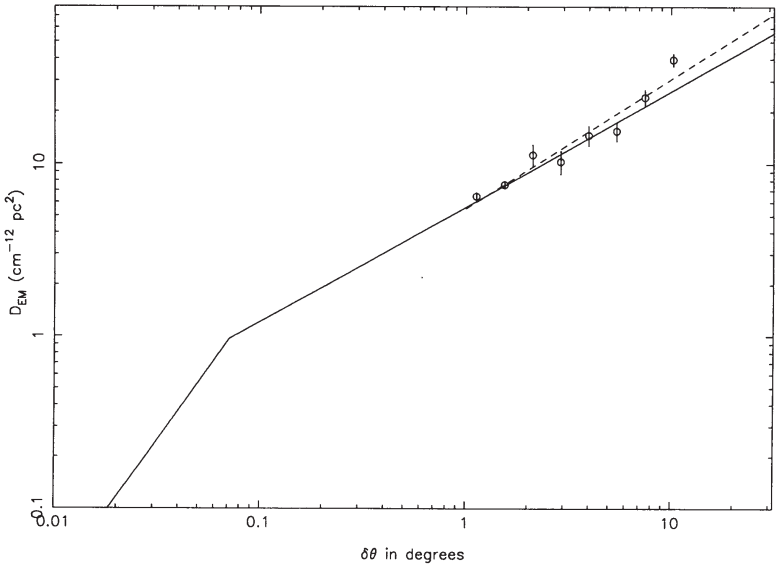

☞ $D_\mathrm{RM},\ D_\mathrm{EM} \propto \begin{cases} \delta\theta^{\frac{5}{3}} & \text{for} \quad \delta\theta < 0.07° \\ \delta\theta^{\frac{2}{3}} & \text{for} \quad \delta\theta > 0.07° \end{cases}$

Power spectrum from extragalactic RMs

Combine measured $\mathrm{RM} = C \int n_\mathrm{e}\, B_\parallel\, ds$ & $\mathrm{EM} = \int n_\mathrm{e}^2\, ds$

to derive power spectra of δn_e and δB separately *(Minter & Spangler 1996)*

☞ $D_\mathrm{RM},\ D_\mathrm{EM} \propto \begin{cases} \delta\theta^{\frac{5}{3}} & \text{for} \quad \delta\theta < 0.07° \\ \delta\theta^{\frac{2}{3}} & \text{for} \quad \delta\theta > 0.07° \end{cases}$

$\Rightarrow \quad E_n,\ E_B \propto \begin{cases} k^{-\frac{5}{3}} & \text{for} \quad \ell < 3.6 \text{ pc} \\ k^{-\frac{2}{3}} & \text{for} \quad 3.6 \text{ pc} < \ell \lesssim 100 \text{ pc} \end{cases}$ (assuming $L = 2.9$ kpc)

$\delta B_\mathrm{rms} \sim 1\ \mu\mathrm{G} \quad \text{for} \quad \ell < 3.6 \text{ pc}$

☞ - True MHD turbulence
- 3D Kolmogorov for $\ell \lesssim 4$ pc & 2D for $\ell \approx (4 - 100)$ pc
- Possibly turbulent sheets / filaments of thickness ~ 4 pc
- Spectral break at $\ell \simeq 3.6$ pc could explain knee in CR spectrum

Outer scale from extragalactic RMs

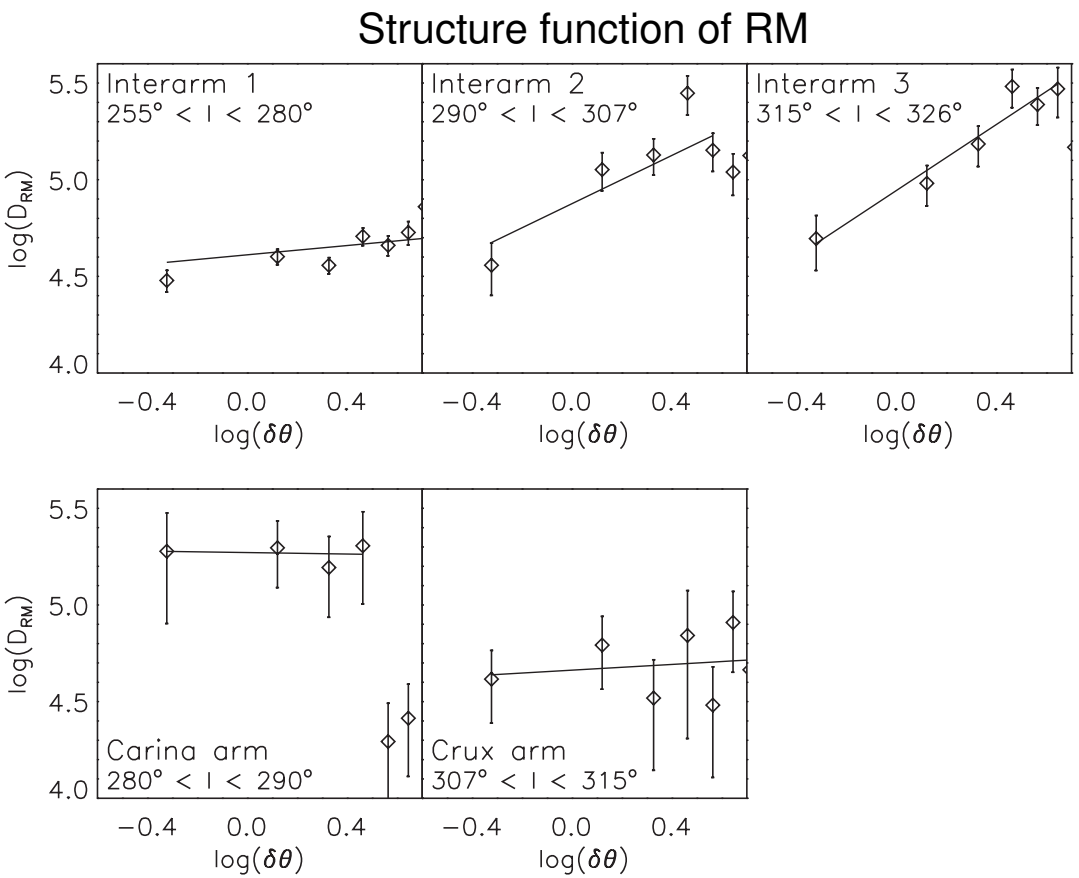

Haverkorn et al. (2008)

- In interarm regions
  - Kolmogorov for $\ell \lesssim$ a few pc
  - Flatter for $\ell \approx$ (a few – 100) pc
  - $\Rightarrow \ell_{\rm out} \sim 100$ pc
- In spiral arms
  - Kolmogorov for $\ell \lesssim$ a few pc
  - Flat for $\ell \gtrsim$ a few pc
  - $\Rightarrow \ell_{\rm out} \sim$ a few pc

Power spectrum from Galactic pulsar RMs

Combine measured $\mathrm{RM} = C \int_0^L n_\mathrm{e}\, B_{\parallel}\, ds$ & $\mathrm{DM} = \int_0^L n_\mathrm{e}\, ds$ & L

to derive power spectrum of δB at large scales *(Han et al. 2004)*

Magnetic energy spectrum

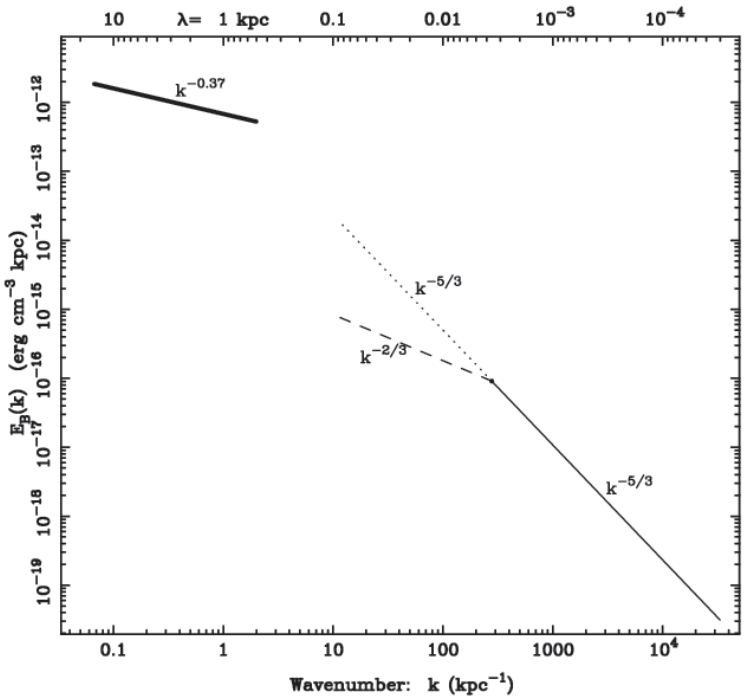

☞ $E_B \propto k^{-0.37}$

for $\ell \approx (0.5 - 15)$ kpc

$\delta B_\mathrm{rms} \sim 6\ \mu\mathrm{G}$

Prospects for RM grids

- Pulsars with measured DMs & RMs
  - Currently : 1 159
    (ATNF pulsar catalogue, version 1.60, *Manchester et al. 2005*$^{+}$)
  - Expected with SKA 1 :
    - Total number : $\sim$ 18 000
    - Density in Galactic plane : $\sim$ 6 deg^{-2}
    (*Keane et al. 2015*)

- Extragalactic sources with measured RMs
  - Currently : $\simeq$ 45 000
    (*Oppermann et al. 2015 + Schnitzeler et al. 2019*)
  - Expected with SKA 1 :
    - Total number : $\sim (1-4) \times 10^7$
    - Average density : $\sim$ (300 - 1 000) deg^{-2}
    (*Haverkorn et al. 2015*)

Outline

1 Dust polarization

2 Faraday rotation

3 Synchrotron emission

4 Faraday tomography

Total & polarized intensities

$\mathcal{E} = f(\alpha)\, n_{\mathrm{CRe}}\, B_\perp{}^{\alpha+1}\, \nu^{-\alpha}$ & $\vec{\mathcal{E}}_{\mathrm{pol}} \perp \vec{B}_\perp$

- Total intensity : $I = \int \mathcal{E}\, ds$ ☞ $B_\perp$ (strength only)

- Polarized intensity : $\vec{P} = \int \vec{\mathcal{E}}_{\mathrm{pol}}\, ds$ ☞ $(\vec{B}_{\mathrm{ord}})_\perp$ (strength & orientation)

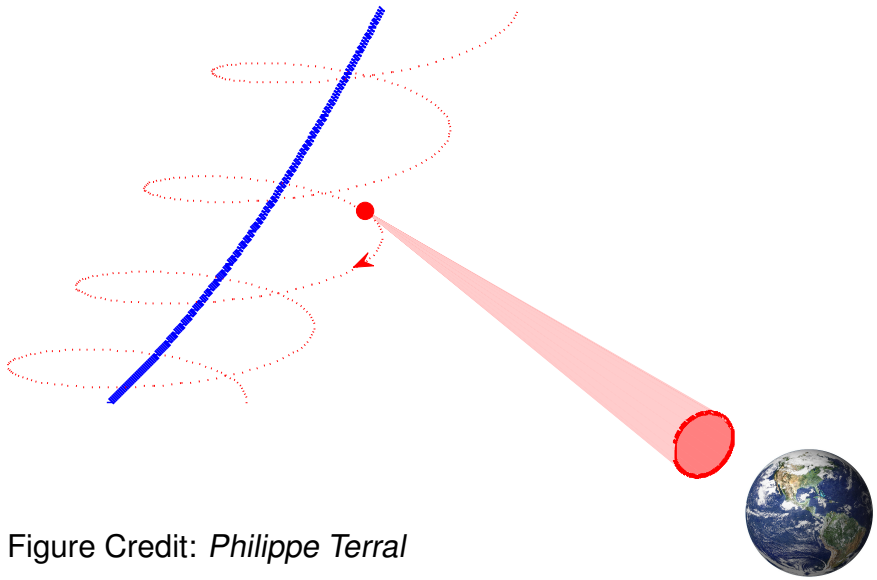

Figure Credit: *Philippe Terral*

Total & polarized intensities

$\mathcal{E} = f(\alpha)\, n_{\mathrm{CRe}}\, B_\perp{}^{\alpha+1}\, \nu^{-\alpha}$ & $\vec{\mathcal{E}}_{\mathrm{pol}} \perp \vec{B}_\perp$

- Total intensity : $I = \int \mathcal{E}\, ds$ ☞ $B_\perp$ (strength only)

- Polarized intensity : $\vec{P} = \int \vec{\mathcal{E}}_{\mathrm{pol}}\, ds$ ☞ $(\vec{B}_{\mathrm{ord}})_\perp$ (strength & orientation)

↳ $Q + i\,U = \int \mathcal{E}_{\mathrm{pol}}\, e^{2i\psi}\, ds$

Total & polarized intensities

$\mathcal{E} = f(\alpha)\, n_{\rm CRe}\, B_\perp{}^{\alpha+1}\, \nu^{-\alpha}$ & $\vec{\mathcal{E}}_{\rm pol} \perp \vec{B}_\perp$

- Total intensity : $I = \int \mathcal{E}\, ds$ ☞ $B_\perp$ (strength only)

- Polarized intensity : $\vec{P} = \int \vec{\mathcal{E}}_{\rm pol}\, ds$ ☞ $(\vec{B}_{\rm ord})_\perp$ (strength & orientation)

TI at 1.4 GHz (25m Stockert + 30m Villa Elisa)

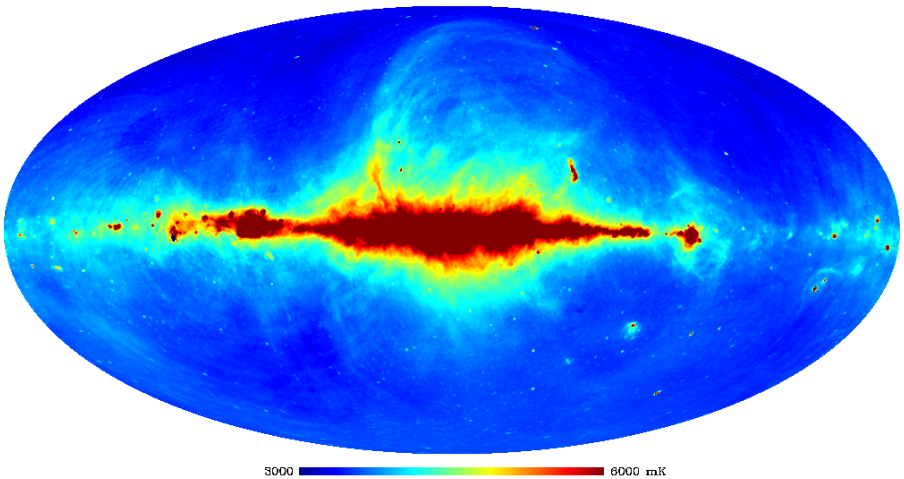

Figure Credit: *Tess Jaffe*

PI at 1.4 GHz (26m DRAO + 30m Villa Elisa)

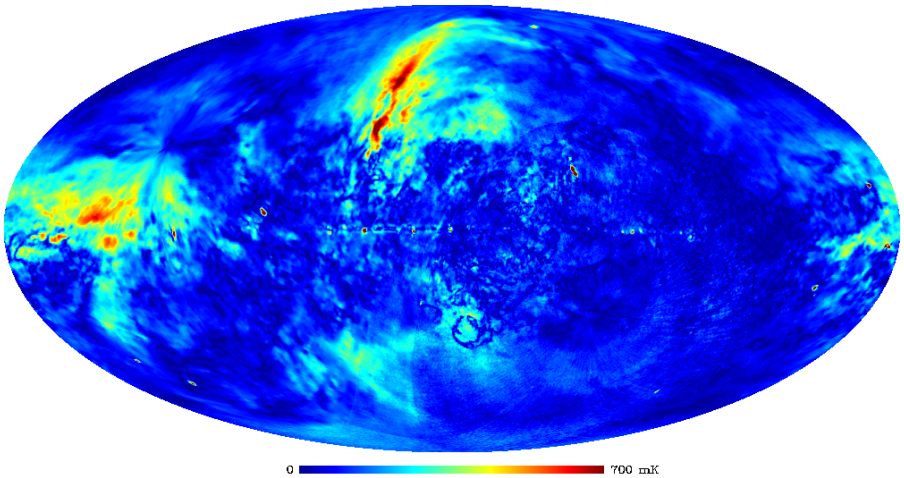

Figure Credit: *Tess Jaffe*

Total & polarized intensities

$\mathcal{E} = f(\alpha)\, n_{\rm CRe}\, B_\perp{}^{\alpha+1}\, \nu^{-\alpha}$ & $\vec{\mathcal{E}}_{\rm pol} \perp \vec{B}_\perp$

- Total intensity : $I = \int \mathcal{E}\, ds$ ☞ $B_\perp$ (strength only)

- Polarized intensity : $\vec{P} = \int \vec{\mathcal{E}}_{\rm pol}\, ds$ ☞ $(\vec{B}_{\rm ord})_\perp$ (strength & orientation)

TI at 1.4 GHz (25m Stockert + 30m Villa Elisa)

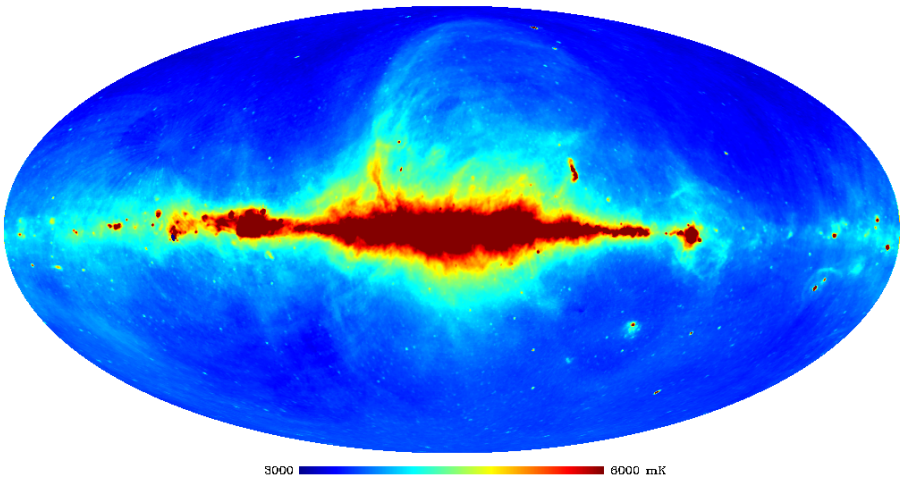

Figure Credit: *Tess Jaffe*

PI & $\vec{B}_\perp$ segtors at 23 GHz (WMAP)

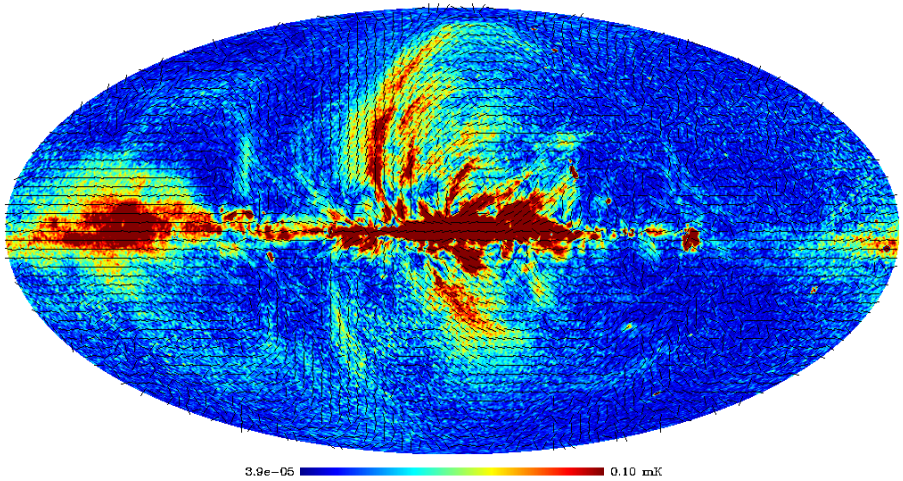

Figure Credit: *Tess Jaffe*

Ordered magnetic field

In general (CR-filled) ISM

- Near the Sun

  - $B_{\rm ord} \simeq 3\ \mu$G vs $B_{\rm tot} \sim 5\ \mu$G

- Global spatial distribution

  - $L_{\rm B} \sim 12$ kpc & $H_{\rm B} \sim 4.5$ kpc

- In the disk

  - $\vec{B}_{\rm ord}$ is horizontal

- In the halo

  - $\vec{B}_{\rm ord}$ has horizontal & vertical components

Fluctuations in *total* intensity

Theoretical developments *(Lazarian & Pogosyan 2012)*
& numerical simulations *(Herron et al. 2016)*

☞ Synchrotron intensity fluctuations are anisotropic, forming filaments $\parallel \vec{B}_\perp$

Synchrotron total intensity map

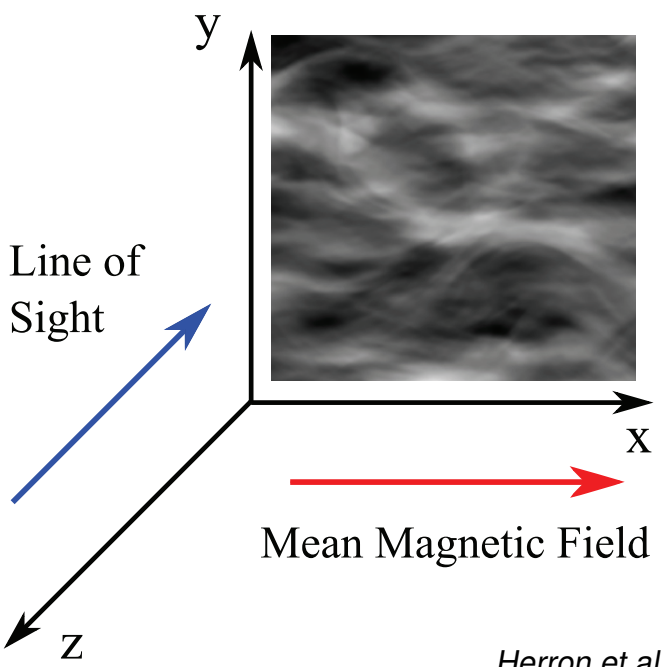

Herron et al. (2016)

Fluctuations in *total* intensity

Synchrotron intensity gradients ☞ orientation of $\vec{B}_\perp$

Synchrotron intensity gradients & polarization vectors (Planck)

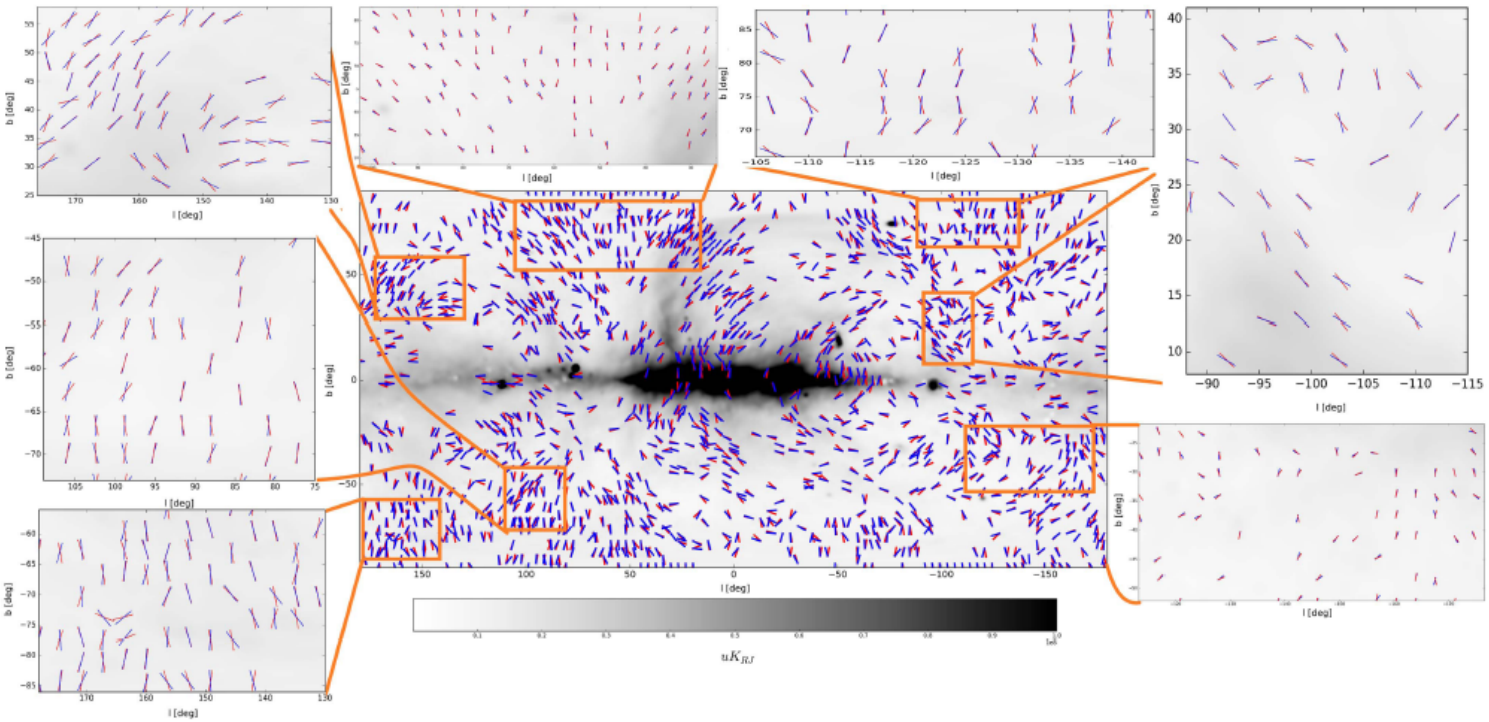

Lazarian et al. (2017)

Fluctuations in *total* intensity

Angular power spectrum of synchrotron intensity

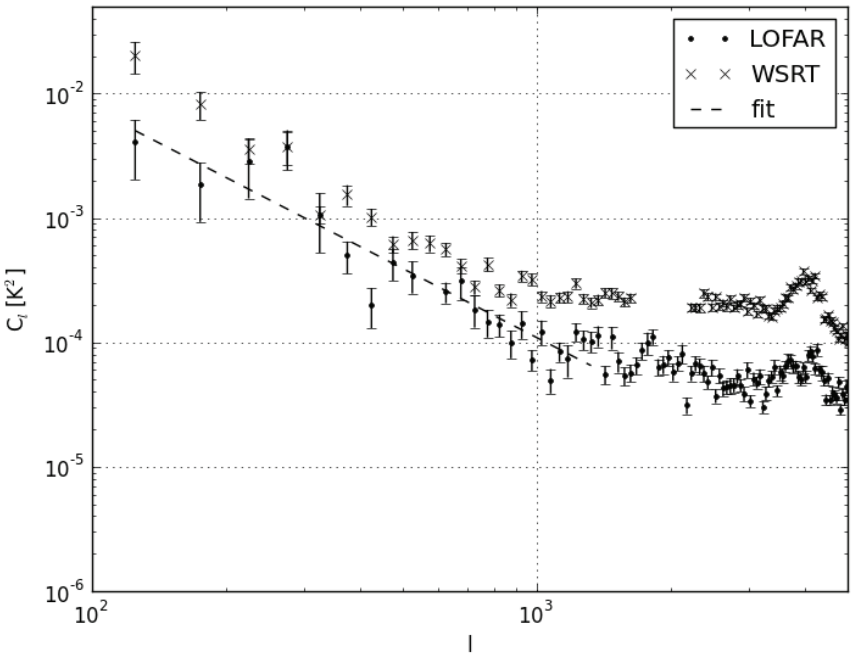

Iacobelli et al. (2013)

☞ $C_l \propto l^{-1.84}$

for $l \approx (100 - 1\,300)$

$\delta\theta \approx (8' - 110')$

$\Rightarrow \ell_{\rm out} \lesssim 20$ pc

$\Rightarrow \dfrac{B_{\rm ord}}{\delta B_{\rm rms}} \lesssim 0.3$

Fluctuations in *polarized* intensity

Total & polarized intensities at 1.4 GHz (ATCA)

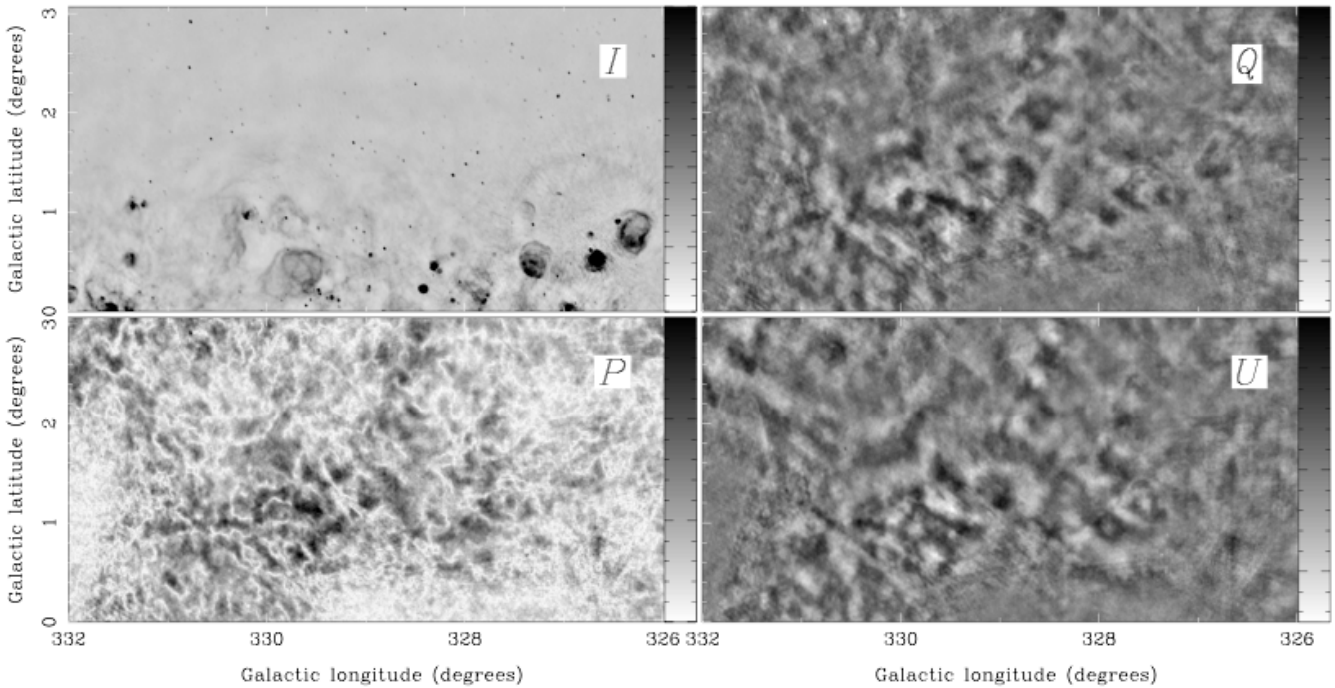

Gaensler et al. (2011)

☞ Filamentary structures in P, with no counterparts in I

- Arise from fluctuations in Faraday rotation
- Probe magneto-ionic turbulence in WIM

Fluctuations in *polarized* intensity

Measure synchrotron polarization gradients

$|\nabla \vec{P}|$ at 1.4 GHz (ATCA)

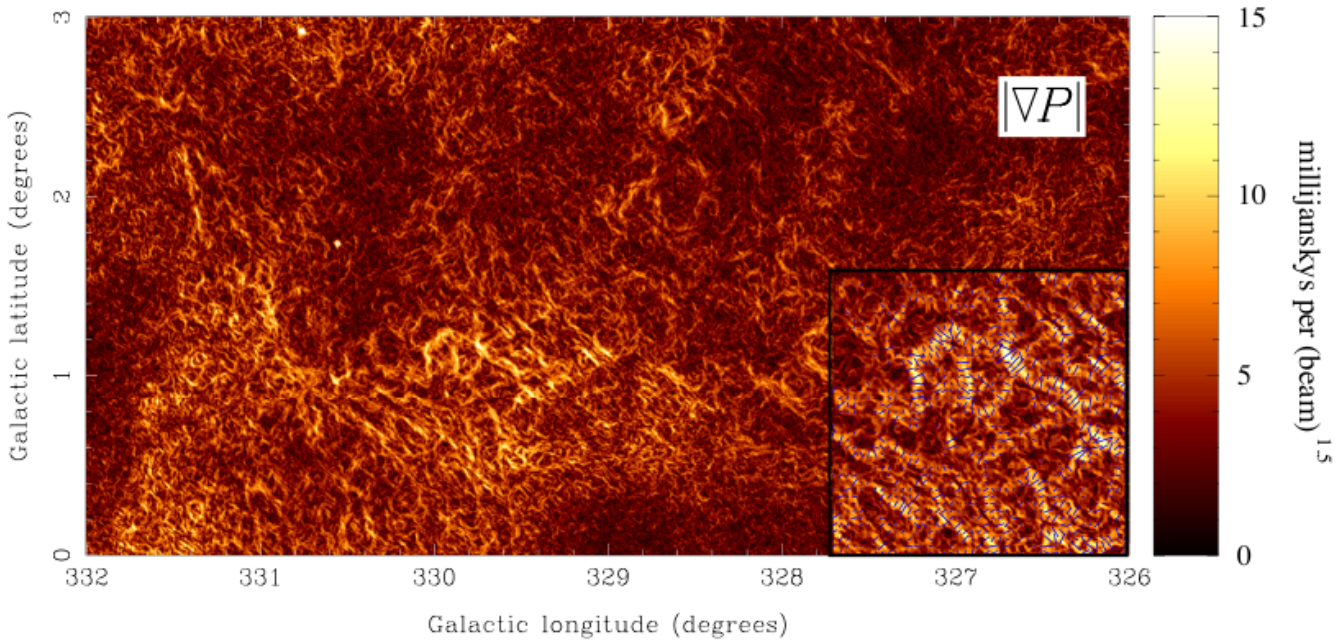

Gaensler et al. (2011)

Compare with 3D MHD simulations

☞ Turbulence in WIM is subsonic or trans-sonic ($\mathcal{M}_s \lesssim 2$) *(Burkhart et al. 2012)*

Fluctuations in *polarized* intensity

- Synchrotron polarization gradients ☞ orientation of $\vec{B}_\perp$
  Measurements at several λ ☞ Info on LOS distribution

Synchrotron polarizat° gradients & polarizat° vectors (from simulat°)

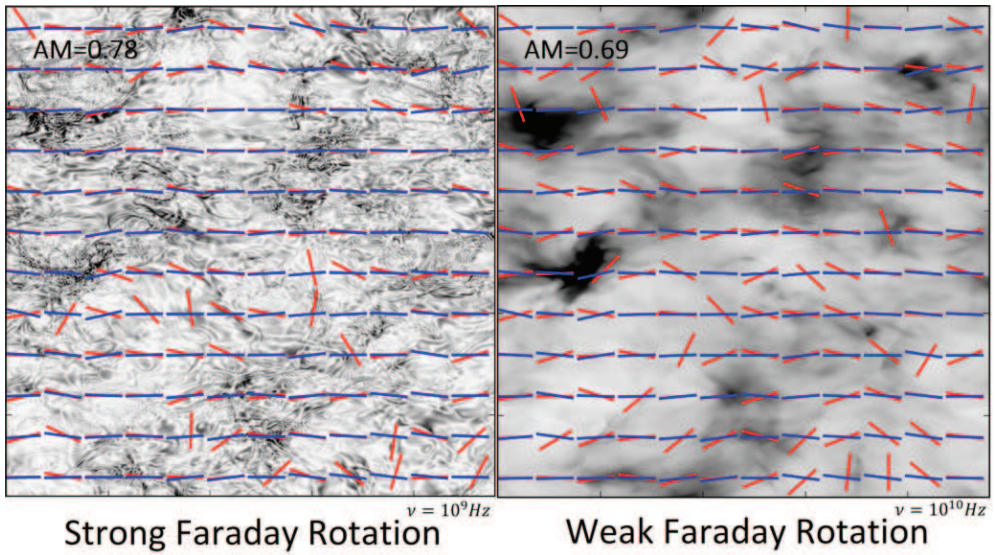

Lazarian & Yuen (2018)

- Gradients of $\frac{dP}{d\lambda^2}$ ☞ $B_\parallel$

Outline

1 Dust polarization

2 Faraday rotation

3 Synchrotron emission

4 Faraday tomography

General concept

- Underlying processes
  - Galactic synchrotron emission : linearly polarized
  - Faraday rotation : λ-dependent
- General idea
  - Measure synchrotron polarized intensity at many different λ
  - Convert λ-dependence into s-dependence
- Output

  Faraday cube = 3D cube of synchrotron polarized emission as fc(α, δ, Φ)

General method

- **Faraday rotation of background source**

$$\Delta\psi = \mathrm{RM}\ \lambda^2 \quad \text{with} \quad \mathrm{RM} = C \int_0^L n_\mathrm{e}\ B_{||}\ ds \quad \text{(rotation measure)}$$

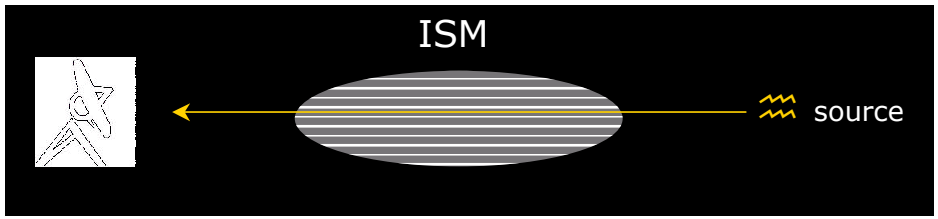

- **Faraday rotation of Galactic synchrotron emission**

Synchrotron emission & Faraday rotation are *spatially mixed*

$$\vec{P}(\lambda^2) = \int \vec{F}(\Phi)\ e^{2i\Phi\lambda^2}\ d\Phi \quad \text{with} \quad \Phi(z) = C \int_0^z n_\mathrm{e}\ B_{||}\ ds \quad \text{(Faraday depth)}$$

☞ Fourier transform of polarized intensity : $\vec{P}(\lambda^2) \rightarrow \vec{F}(\Phi)$

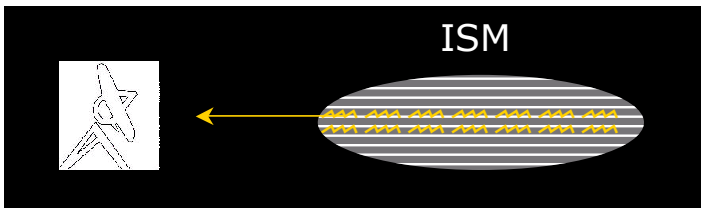

Figure Credit: *Marijke Haverkorn*

Faraday spectrum

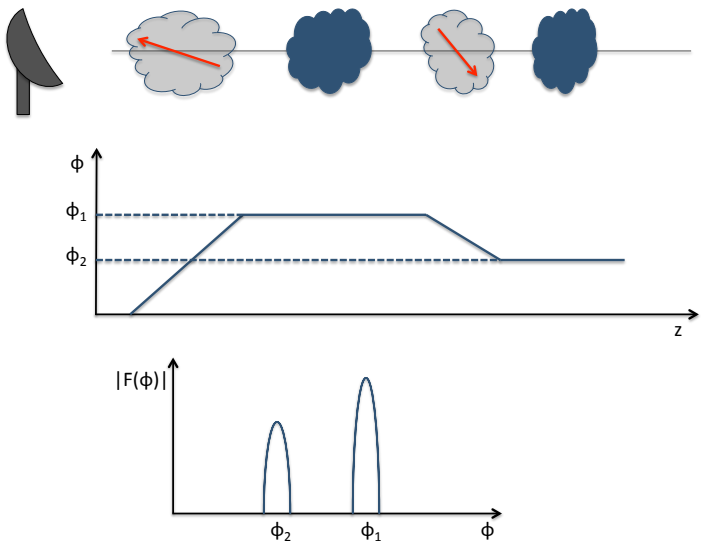

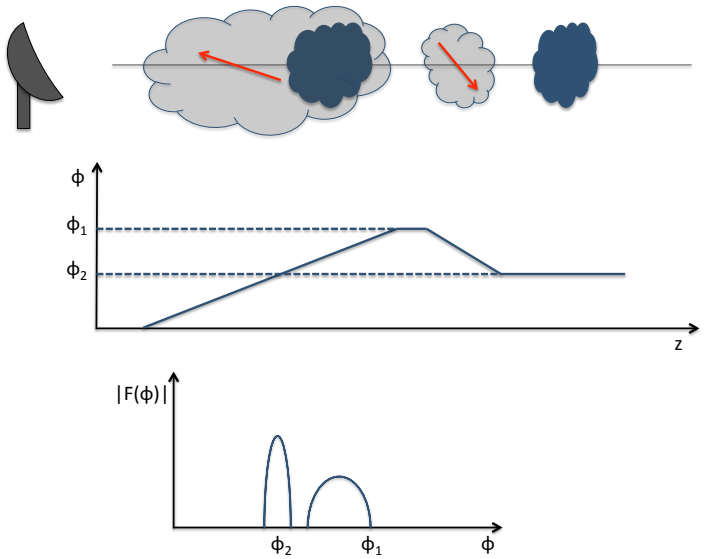

Figure Credit: *Marta Alves*

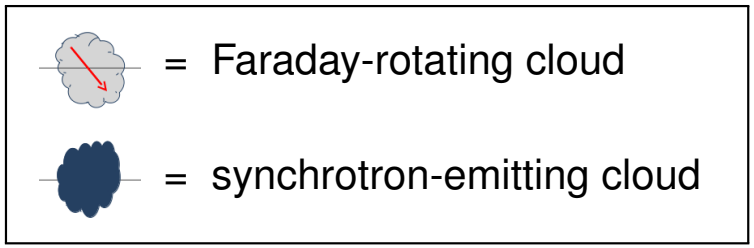

Faraday cube

For given sky area

- Derive Faraday spectrum, $\vec{F}(\Phi)$, in many directions (α, δ)
- Combine all derived Faraday spectra into Faraday cube = 3D cube of $\vec{F}(\alpha, \delta, \Phi)$

Faraday cube toward Fan region, obtained with LOFAR *(van Eck et al. 2017)*

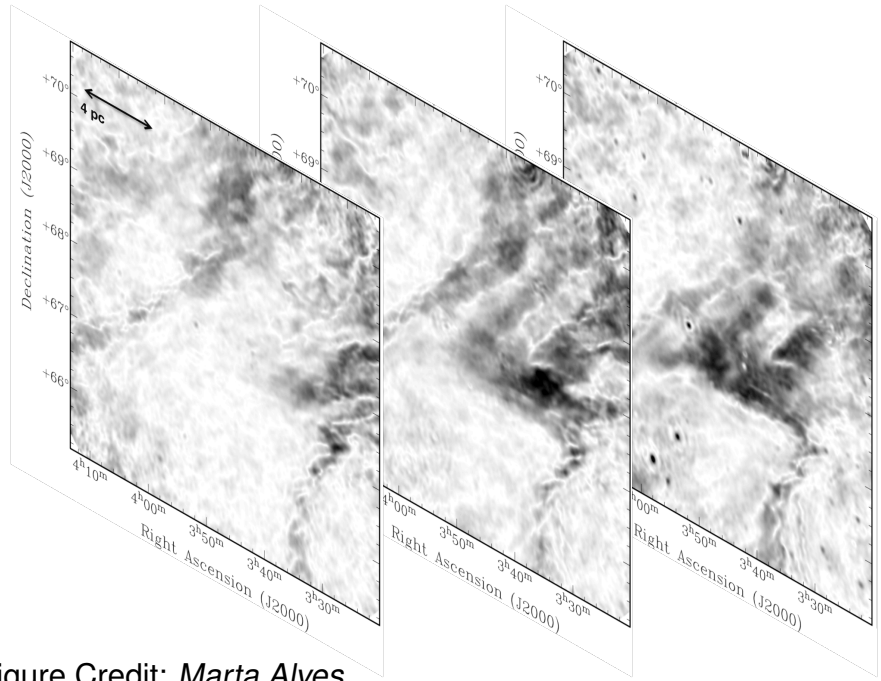

Figure Credit: *Marta Alves*

3 slices at

$$\Phi_1 = -2.0 \text{ rad m}^{-2}$$
$$\Phi_2 = -1.5 \text{ rad m}^{-2}$$
$$\Phi_3 = -1.0 \text{ rad m}^{-2}$$

Example of a nearby magnetized bubble

Polarized intensity at 3 different Faraday depths

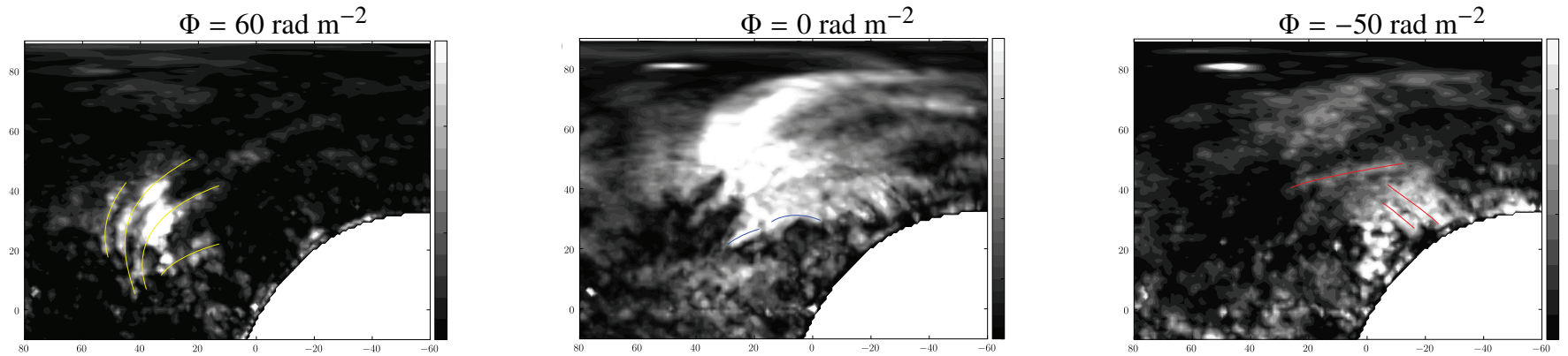

Wolleben et al. (2010)

Interpretation

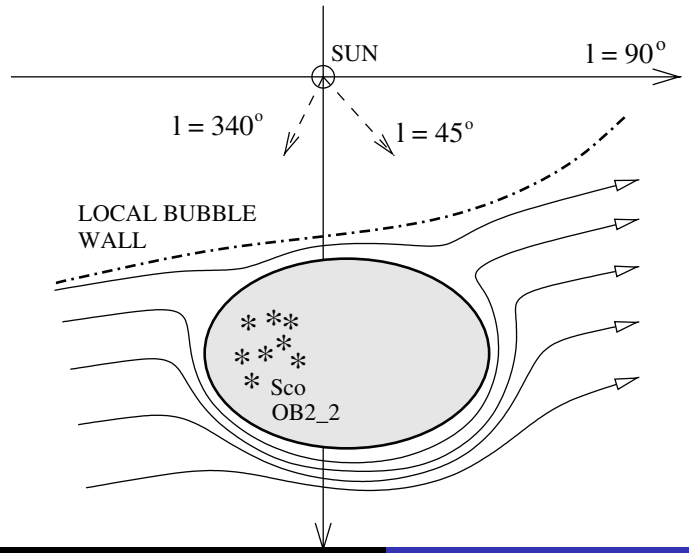

Example of a nearby magnetized bubble

Polarized intensity at 3 different Faraday depths

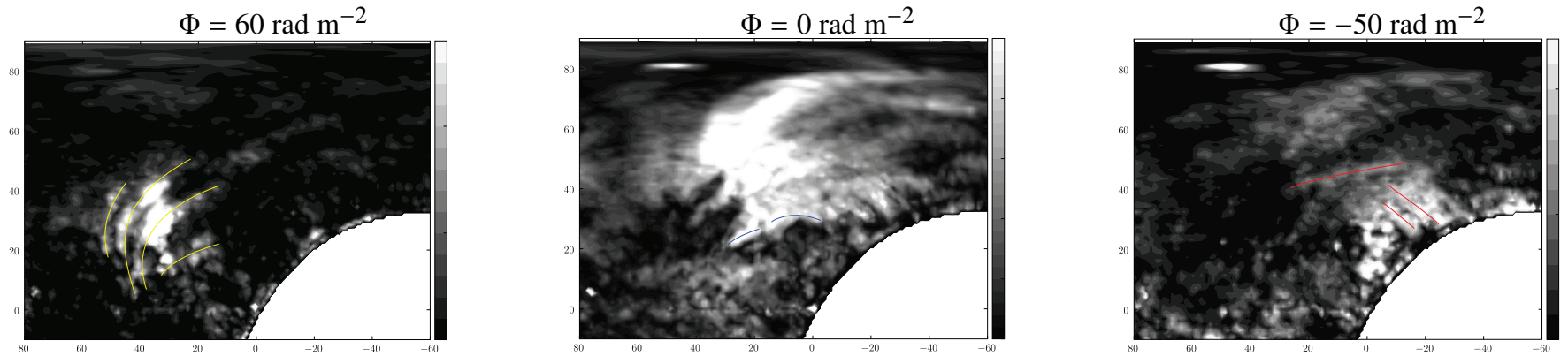

Wolleben et al. (2010)

Interpretation

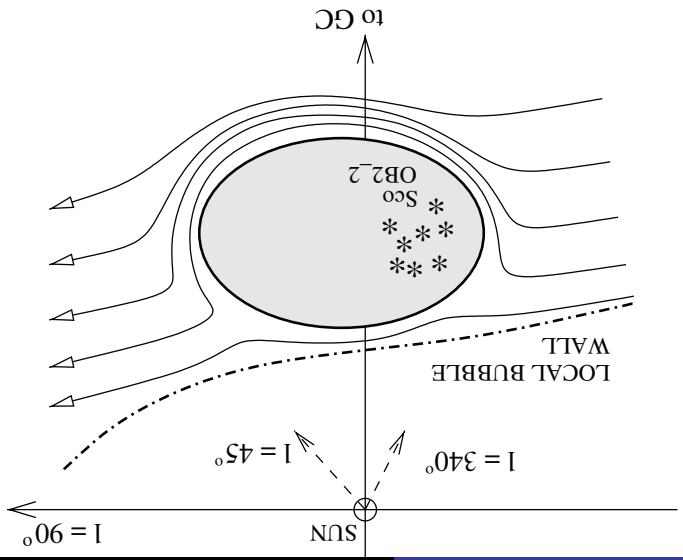

In summary

- From synchrotron polarized intensity map to Faraday cube
  - Measure $\vec{P}(\lambda^2)$ at many different λ
  - Fourier transform $\vec{P}(\lambda^2)$ to obtain $\vec{F}(\Phi)$
- From Faraday cube to physical space
  - Uncover synchrotron-emitting & Faraday-rotating features in Faraday cube
  - Identify these features with interstellar matter structures
- For synchrotron-emitting regions

  $\int \vec{F}(\Phi)\, d\Phi$ ☞ $\vec{B}_\perp$
- For Faraday-rotating regions

  $\Delta\Phi$ ☞ $B_\parallel$